JOURNAL OF OPTOELECTRONICS AND ADVANCED MATERIALS Vol. 12, No. 1, January 2010, p. 85 - 93

Classical holography experiments in digital terms

P. C. LOGOFATU*, F. GAROI, A. SIMA, B. IONITA[a], D. APOSTOL
Laser Dept., National Institute for Laser, Plasma and Radiation Physics PO Box MG-36, 077125, Magurele, Romania
[a]*GSI Helmholtz Centre for Heavy Ion Research GmbH, Planckstrasse 1, D-64291 Darmstadt, Germany*

In this paper we present some classical holographic experiments only this time performed in various digital experimental arrangements. The information of the hologram is either calculated using discrete light diffraction formulae or recorded on a CCD, which takes the place of the registration holographic plate. The information of the hologram may be coded on a SLM which when illuminated reproduces the effects of the diffraction through the hologram or the diffraction may be calculated by a computer and so the output may be obtained more or less digitally. The distinction between virtual and actual digital is stressed. Experiments starting from the simple playback of computer generated Fourier holograms, going through basic interference experiments such as obtaining fringes of equal inclination up to more sophisticated configurations such as Fresnel holograms, are presented with a stress on the digital aspects that make these experiments depart from their classic counterpart.

(Received December 15, 2009; accepted January 20, 2010)

Keywords: Digital holography, Classical holography, Information optics, Digital optics

1. Introduction

The digital revolution inevitably dragged optics in its midst. New tools for the optical physicist such as the Charged Coupled Devices (CCD) and the Spatial Light Modulators (SLM) are now available. The digital holography made its appearance in the sixties when there were no other digital devices besides the computer and it may be credited to Lohmann and Paris [1]. The spectacular increase in computation power and availability of the computers, as well as the invention of hybrid optoelectronic devices such as the CCD and the SLM opened new vistas for the development of digital physical optics and stimulated the theoretical study of discrete optics.

In this paper we present some classical holographic experiments only this time performed in various digital experimental setups. The information of the hologram is either calculated using discrete light diffraction formulae (in which case we use also a virtual or recorded on a CCD, which takes the place of the registration holographic plate. The information of the hologram may be coded on a SLM which when illuminated reproduces the effects of the diffraction through the hologram or the diffraction may be calculated by a computer and so the output may be obtained more or less digitally. Experiments starting from the simple playback of computer generated Fourier holograms, going through basic interference experiments such as obtaining fringes of equal inclination up to more sophisticated configurations such as Fresnel holograms, are presented with a stress on the digital aspects that make these experiments depart from their classic counterpart.

2. Virtual versus actual digital (discrete)

The word digital (or discrete) is often used in different contexts which give it different meanings. The problem goes to the core of digital holography which in fact is a richer concept than first meets the eye. A discussion is necessary for making the distinction between virtual digital and actual digital. Computer simulations are completely on the side of the virtual digital, of course. But a computed generated hologram (CGH) that is physically realized crosses the boundary between virtual digital and actual digital and it may not pass the boundary completely. Because the diffraction of light by a illuminated CGH is preferably calculated in terms of discrete optics, although the option of calculation in terms of continuous optics remains open. The optoelectronic devices such as CCD and SLM are physical and therefore actual digital. However the sampling that is done by the CCD is a discretisation of the recorded hologram. One may calculate rigorously, in continuous terms the diffraction pattern on the CCD surface but what matters is the information captured by the CCD which is discrete and sampled. The information recorded by the CCD may further be processed in a virtual digital way using a computer programme or an actual digital way using a SLM. A SLM tries to represents a discrete sampled hologram and it succeeds to some extend, but, being physical, the field distribution at the SLM surface is continuous, non-discrete. The propagation of the light diffracted by the SLM results in a close approximation of the discrete calculation of the sampled discrete hologram represented on the SLM but there are differences. Actually there are efforts to make the diffraction by the SLM more closely resembling the intended discretisated output [2]. But some differences are insurmountable. The diffraction on a SLM will always have diffraction orders due to its periodicity, for instance.

As one can see the problem is not simple. We have shown that the distinction between virtual and actual digital should be made but also we discovered along the way that this distinction is not very clear cut. All elements of a holographic experiment, the input object and the reference, the recorded hologram, the hologram used for reconstruction and the output object may be real continuous, actual digital and virtual digital, sometimes only pending on a subjective point of view and not being an intrinsic quality of the element. This goes to the very core of the problem of the correspondence between real continuous physical phenomenon and its digital, discrete model used in computation. Lohmann and Paris were careful to take into consideration the digital perturbation in the physical diffraction [1] but we are still far from having established on solid theoretical grounds the correspondence in question. We tried to do it in reference [3] but only at a very simple level just for the discrete Fourier transform, and we pointed out the correspondence problem in reference [4].

3. Classical holography experiments in digital terms

Our research group, Laser Interferometry and Applications, from the National Institute for Laser, Plasma and Radiation Physics, has an extensive experience in holography that spans decades [4-10].

We think is appropriate at this point to give some details about the equipment we used in the experiments. Some of the details that follow can be seen in Fig. 1. The special optoelectronic digital components in the arrangement are a Sony XCL-X700 CCD camera with 1024×768 pixels of 4.65 μm pitch horizontally and vertically, working at a sampling rate of 30 fps and a phase only HEO1080P SLM from HoloEye, working on reflection, with a resolution of 1920×1080 pixels of 8 μm pitch horizontally and vertically, which corresponds to a 15.36×8.64 mm active area, with a refresh rate of 60 Hz. As a light source in the recording part of the holographic process we used a He-Ne laser, 632.8 nm wavelength (red light). As alight source in the reconstruction part we used a solid-state YAG-ND diode pumped laser of 532 nm wavelength (double the original frequency, green light).

The optoelectronic devices we used, the CCD and the SLM, are not necessary for performing digital holography. But they are if you want to perform all-actual digital holography, and to avoid emulating the physical diffraction process, whose simulation is always less than perfect, to say the least. What is essential to all-actual digital holography is the fact that instead of photographic plates, a CCD and a SLM are used instead. They play the two different parts that the holographic plate plays in classical holography experiment, a recording medium and the critical element of the reconstruction process, the one which contains the information that can be decoded by diffraction. The photographic plate is, of course, in two distinct states when it performs these two distinct tasks. For the recording purposes is blank, unexposed, containing no information. For the reconstruction purposes is a developed photographic plate containing the interference figure created by the reference and the object waves. To be able to perform the two distinct tasks with two different elements is a tremendous advantage. It permits real-time reconstruction of the holographic image, i.e. the two stages of the holographic process can be performed simultaneously. We skip the messy, lengthy chemical intermediary process of developing the hologram. The ability of merging the two stages of recording and reconstruction into one is of critical important especially for holographic interferometry, because allows for real-time, in situ monitoring.

Holography is already interferometry. However there is such a thing as holographic interferometry where two holograms are made to interfere among themselves. Therefore it seemed appropriate to include beside the holographic experiments of single interferometry presented in section 3.1-3.3 to talk also of double interferometry holographic experiments in subsections 3.4-3.5. It is particularly important to include holographic interferometry experiments in this article because it is in interferometry that the full advantage of the all-actual digital holography of merging the two stages of holography into one becomes apparent and proves extremely useful. Namely we are able to perform real-time in situ monitoring of the modifications suffered by the object used in the recording process, which is the studied object in holographic interferometry. Of course, one may object that computers are fast nowadays and fast algorithms for digital calculus are available so that a hybrid experiment, partial-actual and partial-virtual digital in which the reconstruction part is done virtually is equally valid for real-time experiment purposes. to some extent this is true. However, as we said, digital calculation emulates only imperfectly the physical diffraction process. As for the computation speed, no computer does it faster than Mother Nature.

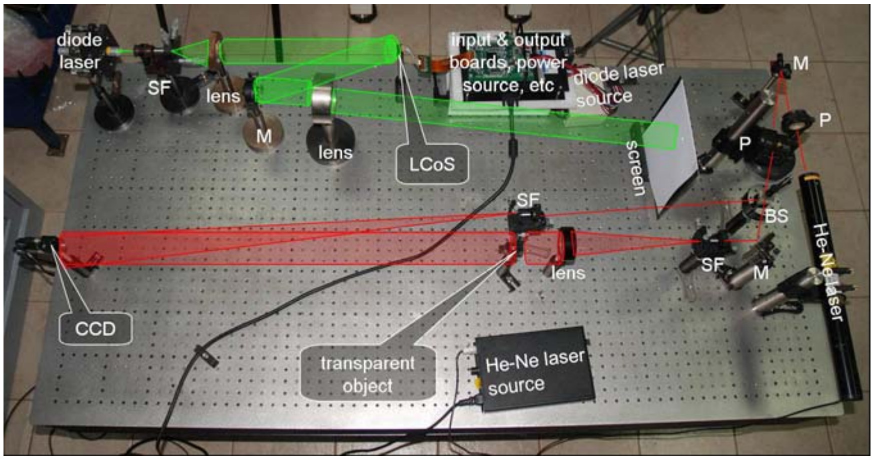

Fig. 1 Experimental arrangement for digital lensless Fourier holography. The following short-hand notations were used: "P" for polarizers, "M" for mirrors, "BS" for beam-splitter, "SF" for spatial filter, "LCoS" for liquid crystal on silicon and "CCD" for charged coupled devices. The part where the red light from the He-Ne laser propagates is the registration part of the holographic process. The part where the green light from the diode laser propagates is the reconstruction or the playback part of the holographic process.

a

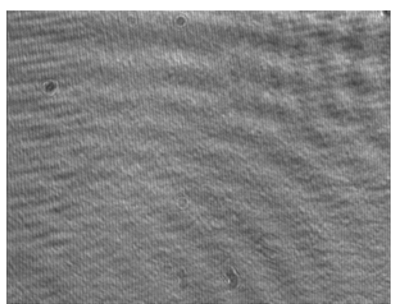

b

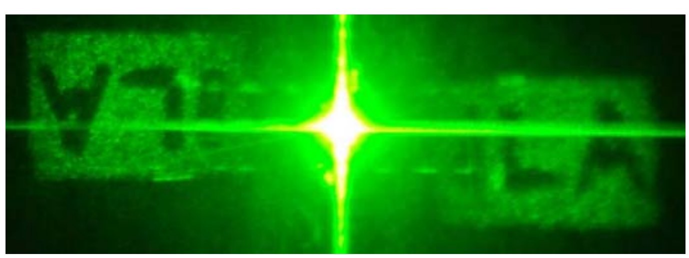

c

Fig. 2. Stages of the holographic process in this particular case of the Fraunhofer-Fourier lensless holography: (a): Input image (transparency); (b) Recorded hologram (on the CCD); (c) Reconstructed image. Part (b) does not look much but it contains encoded in fringes of interference the information of (a). In (c) we can see both the virtual and the real image object focalized in the same plane (the screen) by the corresponding lens because it is a Fourier hologram.

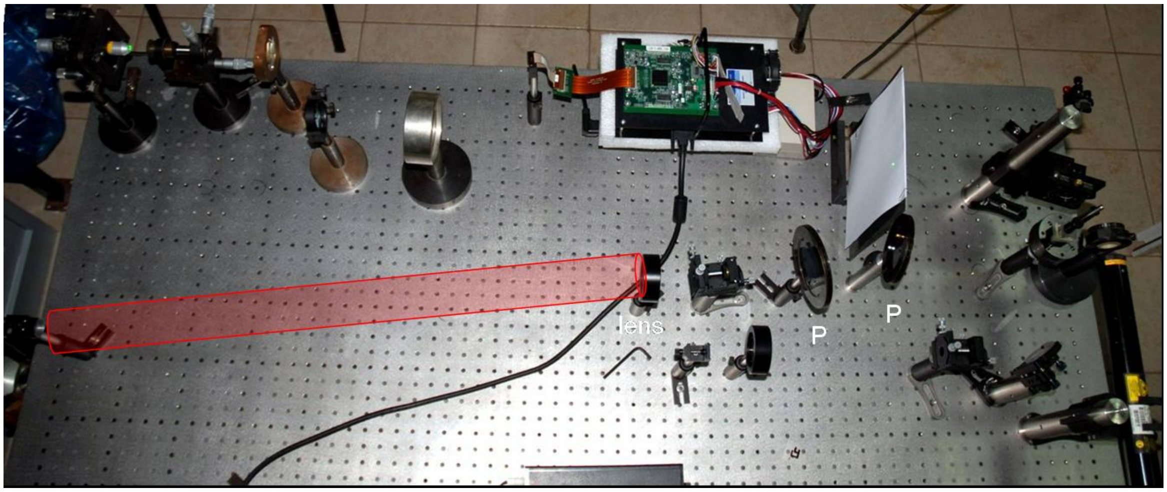

Fig. 3. The experimental arrangement for Fresnel holography. The only notable difference in this *arrangement compared to Fig. 1 is that the reference is a plane wave instead of spherical wave.*

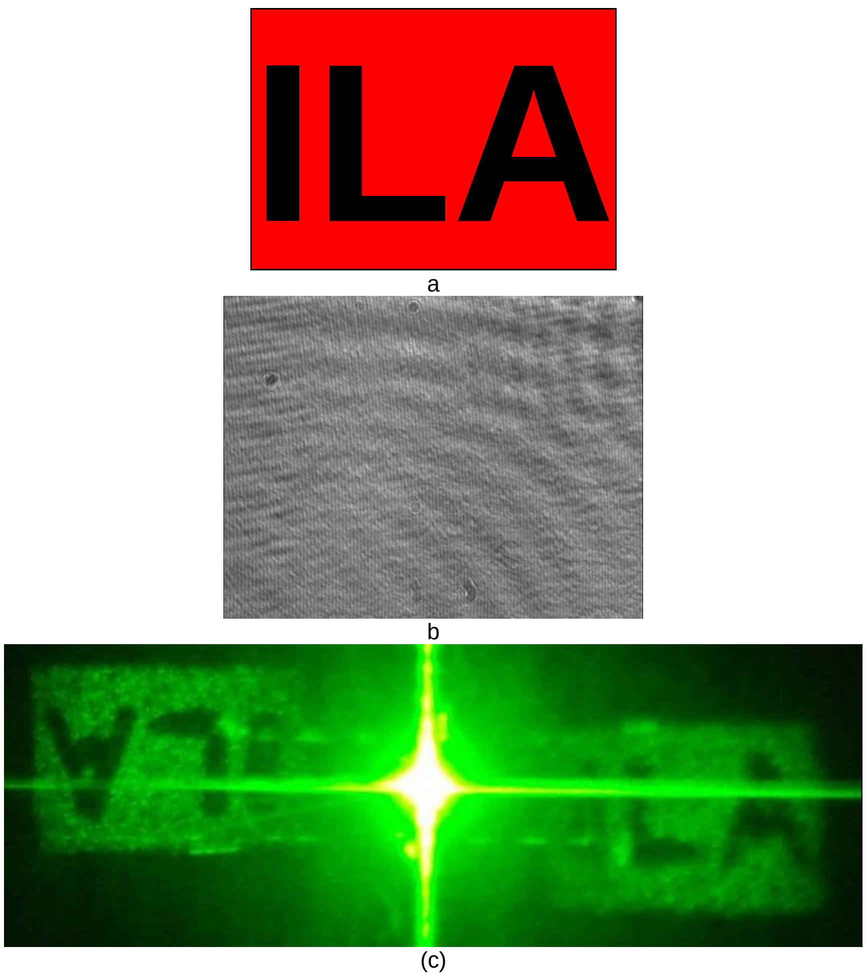

Fig.4. Stages of the holographic process in this particular case of the Fraunhofer-Fourier lensless holography: (a): Object image (transparency); (b) Recorded hologram (on the CCD); (c) Reconstructed image. One may not distinguish much difference between part (c) of this figure and part (c) of Fig. 2 except that the virtual and the real image are focused at different depths, as opposed to the case of Fourier holograms

3.1 All-actual digital lensless Fourier holography

There are two types of Fourier holograms those which use a lens for the realization of the Fourier transform in the hologram plane where is recorded with the help of a plane reference wave, or those which do not use a lens (hence the name lensless) that instead record the Fresnel transform of the input but with the help of a spherical reference wave with the origin situated with the input in a plane parallel to the holographic plate. It is known that the quadratic phase factor brought by the Fresnel transform is nullified in this way by the spherical quadratic phase of the reference [11].

In Fig. 1 is represented the bivalent experimental arrangement we used to perform the digital holography experiment. It serves two purposes: to record holograms and to reconstruct them. The hologram formed by the interference of the diffraction from the diffusive object and the collimated beam from the lower side of the Fig. 1. is recorded by the CCD. For both the light source is a the He-Ne laser. The hologram, converted into a phase distribution, is then modulated in the pixels of the SLM. The upper collimated beam reconstructs the hologram. This beam comes from the second light source, the diode laser. The fact that the two sources of light in use (lasers) are of different wavelength as well as the different dimensions of the CCD and SLM pixels is bound to create some problems in the reconstruction stage, but on the other hand this also emphasizes the bivalence of the arrangement and its flexibility, which could not be attained with a classical holographic arrangement. Actually the two stages of the experiment are quite independent and only the computer that controls them makes the connection between them. This connection, however, allows the monitoring in real-time of changes of the diffusive object. In classic terms it is the equivalent of an uninterrupted series of instantaneous development and reconstruction of holograms.

A digital Fraunhofer-Fourier hologram is the intensity distribution of the Fourier transform of the optical field of the object. Since our SLM is phase only, we convert intensity in phase, which is the classical equivalent of bleaching the hologram. The playback of the phase hologram modulated by the computer Fourier transformed through a lens reconstructs quite accurately the object. Improvement of the image may be obtained here, as in any other instances where either the intensity or the phase cannot be modulated by using an iterative Fourier transform approach (IFTA). The IFTA iterative algorithm is made possible by the fact that generally the phase distribution of the object does not matter, it is arbitrary and we can change it as we wish as long as it is sufficiently random to prevent coherent spurious effects. For more information see reference [2].

Of course, as we mentioned before, we could wave replaced the second part of the holographic experiment by computer calculation, and we actually did the experiment in this fashion earlier [10]. We also presented the objections to such and approach and that is why we consider the present work a step up compared to the past work shown in [10].

3.2 All-actual digital Fresnel holography

Another experiment was the creation of a Fresnel hologram. This experiment, more than the others is inconvenienced by the incongruity between the recording and the reconstruction sections respectively. Generally the holographic recording plates have higher resolution and recording and playback area than the CCDs and the SLMs. But there is one aspect where classical holography cannot beat digital holography, namely the possibility of creating holograms that can be reconstructed instantly. This is the essence of the bivalence of the experimental arrangement built to execute almost simultaneously the recording and the playback of holograms.

In Fig. 3 it is shown an experimental arrangement for all-actual digital holography. It is quite similar to the arrangement shown in Fig. 1 except that the reference wave is now spherical. The consequence of this is that the virtual and the real output image are not focalized by the lens at the same depth, although due to the specific conditions of digital holography such as small relative size of the input object compared to record, small absolute size of input object, the difference of depth is small. Still, one can notice in Fig. 4 that the two output objects are focused at different depths, and one of them looks more focused on the projecting screen than the other (see Fig.4c).

3.3 All-virtual digital ghost holography

One does not need at all the physical reality for making holography. All can be done virtually in the computer. In this subsection we take the classical holography experiment of ghost Fresnel holograms. The input is made up of two images, the letters **L** and **O** and both of them can play the role of object or reference. The hologram is computed using discrete Fresnel transform and we retain from the result only the intensity information (i.e. we calculate its squared absolute values). We could reproduce graphically the hologram but there is no point in doing that since it looks completely uninteresting, like random speckle. There is order in the apparently random speckle but this order become apparent only when we illuminate the hologram with the proper reference. In this case the proper reference is either of the letters **L** and **O** but alone this time. If we illuminate the hologram with **O** as reference in the output plane we notice the reference all right but also a ghost-like image of the letter **L**, which here plays the role of the object, as one can see in Fig. 5a. (Of course, by "illuminating the hologram and observing the effect in the output plan" means here calculating the Fresnel transform of the hologram transmittance pattern multiplied with the light field distribution generated by the input by Fresnel-type diffraction in the hologram plane and then taking the absolute squared values of the output and this final results is what is illustrated in Fig. 5a.) In Fig. 5b we have, of course the reciprocal of Fig. 5a, with L playing the role of reference in O being the object and the ghost.

It should be noted that the ghost-like appearance of the object is due to the fact that another object is not a proper reference and cannot produce a hologram able to reconstruct with accurate details the object in the output plan. The reference provided by another object is not uniform in the hologram plane and therefore not all the parts of the field diffracted by the object are coded in high contrast interference fringes. These parts of the diffracted field of the object will not contribute to the reconstruction of the object image and hence this image will look poorly in the output plane.

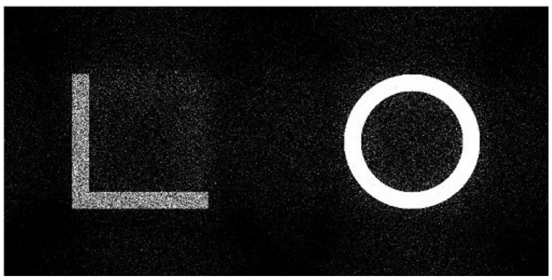

(a)

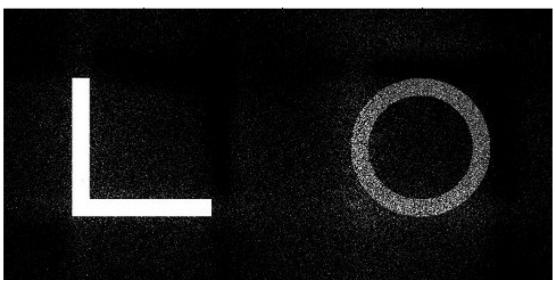

(b)

Fig. 5. The hologram obtained from the interference of the fields generated by **L** *and* **O** *is in turn illuminated with* **O** *(a) and* **L** *(b) used as references and in the output one may notice beside the reference a ghostlike image of the corresponding object.*

3.4 Holographic interferometry of lateral displacement

As we already pointed out, holography already is interferometry. However the waves diffracted by two slightly different holograms recorded in the same material may interfere in their turn. One such slight difference could be a lateral displacement. If we record twice on the same holographic recording material (photographic plate or CCD) and then we playback the double exposed hologram we will notice that the object image in the output is striated by fringes perpendicular to displacement direction (see Fig. 5). The density of the fringes depends on the magnitude of the displacement and actually we can infer the magnitude from the density. It is in essence the principle of Young interference, between two coherent points situated at a small distance in the transversal plane. Each point of the original hologram interferes with itself and the larger the displacement between slits, the smaller the distances between fringes. It is basically an experiment about spatial coherence.

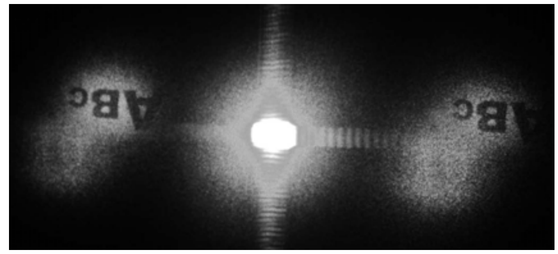

(a)

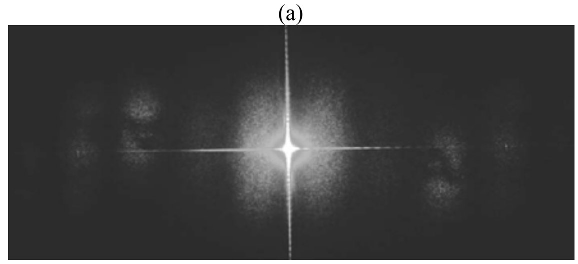

(b)

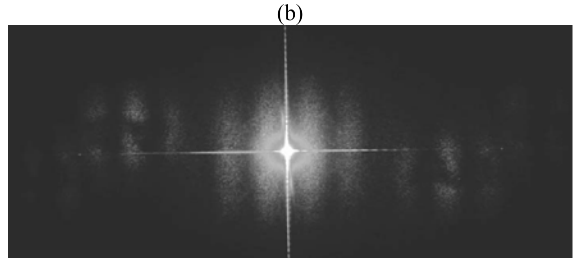

(c)

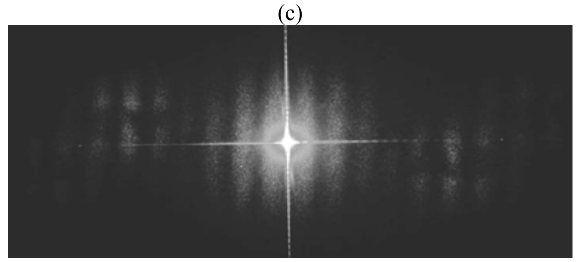

(d)

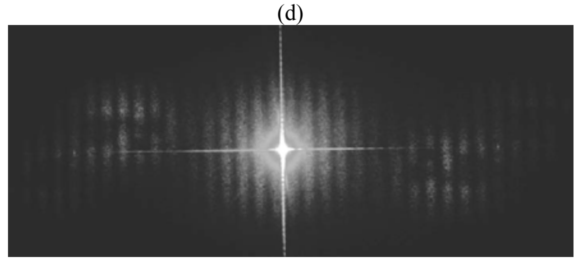

(e)

Fig. 5 The output from the reference hologram (a) and the results of the interference between the original hologram and holograms displaced horizontally with 2 μm (b), 3 μm (c), 4 μm (d) and 6 μm (e) respectively.

Indeed, if in the usual conditions, by which we mean using the same hologram and wavelength both for recording and reconstruction, the relation between the lateral displacement d and the interfringe i observed on the screen would be

$$\Lambda = f\,\lambda/d\ , \tag{1}$$

where f is the focal length of the lens used to from the image on the screen, in the present conditions where we have a laser of wavelength λ_R=632.8 nm for recording and a laser of wavelength λ_G=512 nm for reconstruction, and the initial hologram is magnified due to the unequal pitch of the CCD and the SLM with a factor p_G/p_R, where, obviously, p_R=4.65 μm is the pitch of the CCD, and p_G=8 μm is the pitch of the SLM, relation (1) takes a more complicated form. First let us write the equivalent of (1) in our conditions,

$$\Lambda_G = f\,\lambda_G/d_G\ , \tag{2}$$

where Λ_G is the interfringe measured on the green interference figure on the reconstruction screen and d_G is the apparent displacement of the input object that would create the magnified hologram on the SLM using the green laser. In order to find out the relation between the apparent displacement d_G and the real displacement d, the one that interests us, we have to go further back to the basic principles of holography and even further to diffraction of light [12]. The transparency or the phase distribution of a hologram is of the form

$$H(x,y)\propto\left|a_R(x,y)+a_O(x,y)\right|^2, \tag{3}$$

where a_R and a_O are the reference and the input object waves at the surface of the hologram. (Any multiplicative or additive constant that should be added to (3) and the following equations for rigorousness would not change the conclusions.) The term that is useful for image reconstruction is $a_R^{*}a_O$. The idea is that illuminating the hologram with the same reference wave a_R the reference is canceled out and only the term produced by the input object a_O remains. The original reference used in the recording has the form

$$a_R(x,y)=A_R\exp(-i\,2\pi/\lambda_R\sin\theta\,x). \tag{4}$$

The reference we use on the reconstruction has the wavelenght λ_G and the coordinate x is rescaled with p_R/p_G. In order to cancel out the original reference we have to modify the incidence angle θ so that to compensate for the change of the wavelength. An angle θ_G fulfilling the relation

$$\sin\theta_G/\lambda_G=\sin\theta/\lambda_R\;p_R/p_G \tag{5}$$

will do the job. Now the original distribution produced at the CCD surface by the input object $a_O(x,y)$ appears expanded at the SLM surface by the factor p_G/p_R

$$a_{OG}(x,y)=a_O(x\,p_R/p_G\,,y\,p_R/p_G). \tag{6}$$

We know from the Fresnel diffraction formula that a_O is produced by an input object field distribution $U(\xi,\upsilon)$ the following way

$$\begin{aligned}&a_O(x,y)\propto\int_{-\infty}^{\infty}d\xi\int_{-\infty}^{\infty}d\upsilon\,U(\xi,\upsilon)\times\\&\exp\left\{-\frac{i\pi}{\lambda_R z}\left[(x-\xi)^2+(y-\upsilon)^2\right]\right\}\end{aligned}, \tag{7}$$

where z is the distance from the object U to the recording plane. Consequently a_{OG} has the form

$$\begin{aligned}&a_{OG}(x,y)=a_O(x\,p_R/p_G\,,y\,p_R/p_G)\propto\\&\int_{-\infty}^{\infty}d\xi\int_{-\infty}^{\infty}d\upsilon\,U(\xi,\upsilon)\times\\&\exp\left\{-\frac{i\pi}{\lambda_R z}\left[\left(x\frac{p_R}{p_G}-\xi\right)^2+\left(y\frac{p_R}{p_G}-\upsilon\right)^2\right]\right\}\end{aligned}. \tag{8}$$

Now we ask the question what kind of distribution U can produce a distribution a_{OG} in combination with the green laser wavelength λ_G. Let us introduce a new set of coordinates

$$\xi'=\xi\,p_G/p_R\,,\quad \upsilon'=\upsilon'\,p_G/p_R\,. \tag{9}$$

Replacing the new coordinates in (8) we obtain

$$\begin{aligned}&a_{OG}(x,y)\propto\int_{-\infty}^{\infty}d\xi'\int_{-\infty}^{\infty}d\upsilon' U\left(\xi'\frac{p_R}{p_G},\upsilon'\frac{p_R}{p_G}\right)\times\\&\exp\left\{-\frac{i\pi}{\lambda_G}\frac{\lambda_G}{z\lambda_R}\left(\frac{p_R}{p_G}\right)^2\left[(x-\xi')^2+(y-\upsilon')^2\right]\right\}\end{aligned}. \tag{10}$$

The meaning of Eq. (10) is that the distribution a_{OG} could be created by an input object similar to the original one but magnified with the factor p_G/p_R and situated at a considerably larger distance than the original one, namely

$$z_G = z\frac{\lambda_R}{\lambda_G}\left(\frac{p_G}{p_R}\right)^2. \tag{11}$$

The most important result that we can infer from Eq. (10) is that the apparent displacement d_G that caused interference in the screen is related to the real displacement d simply by the magnifying factor p_G/p_R. Introducing this information in Eq. (2) we finally obtain the relation between the observed interfringe Λ_G and the displacement d

$$d=\frac{f\,\lambda_G\,p_G}{\Lambda_G\,p_R}. \tag{12}$$

For the experiment we used the same arrangement as in subsection 3.2, except this time we needed a special computer program to process the data in order to have an interference figure on the screen. The program first records the original holograms to which we will report later. Then it performs the same procedure for every new frame it captures: it subtracts the intensities values newly acquired from the intensity values of the original hologram, adds a constant to eliminate negative values, usually no more than 128 and then sends the matrix of values thus calculated to the SLM and we can see the results in Figs. 5.b-e.

There is an interesting remark to be made related to the computer processing of the intensity values of the two holograms that interfere, namely that it is very hard to follow how through these transformations the original information about the input object is kept such that in the reconstruction stage the simple illumination of the reference reveals it. This is the beauty of holography and of the light diffraction phenomenon that if the information is stored, albeit in codified form, light will find a way to decode it and reveal it through diffraction. Something similar can be said also about the ghost hologram experiment from subsection 3.3.

3.5 Fringes of equal inclination created by holographic interference

Another experiment that we recreated in digital terms is the interference of two object-images of a diffusing object with a slight offset. After the double recording of the two objects, their reconstructed images interfere creating circular fringes, or fringes of equal inclination, or Heidinger fringes. This is not the first time that we attempted this experiment in our lab. Long ago [7] we performed the experiment in analogous conditions, with holographic plates as recording media. However this time the low resolution of CCD and SLM compared to the resolution of photographic plates, made difficult the digital realization of the experiment, at least for the time being. We found out however that we can contribute with something to the topic, namely a new demonstration of the formation of the Heidinger fringes, one more formal and more rigorous, though less elegant, simple and intuitive than the one presented in reference [7]. Since such a demonstration is not properly part of the topic of the present article we showed the demonstration in the appendix.

It should be noted that this type of interference, that produces fringes of equal inclination is the complement of the experiment presented in subsection 3.4, the interference due to spatial coherence. Here we deal with temporal coherence. The source of light that interfere are separated on the longitudinal axis, therefore they are separated in time. This experiment can be successful only if the temporal coherence, or the coherence longitudinal distance, is large enough.

4. Conclusion

In this paper we presented some classical holographic experiments in digital terms. We made the distinction, not stressed before to our knowledge, between actual-digital and virtual-digital and the fact that this is not necessarily an intrinsic property of the element or the process analyzed but it may be the result of a certain perspective. The defining characteristic of the all-actual digital holography is, with these reserves, the complete replacement of the photographic plate with other physical devices, namely the CCD in the recording stage and the SLM in the reconstruction stage. The main advantage of the all-actual digital holography compared to a hybrid version that leaves the reconstruction stage completely in the hands of the computer, is not just the increased correctness of the diffraction computation and the avoidance of some digital side-effects, but even an increased computation speed.

Appendix A. Holographic circular fringes obtained by longitudinal displacement of a diffusing plane object (Heidinger)

We record twice on the same recording medium the Fresnel hologram of a diffusing planar object $U(\xi,\upsilon)$ situated in two positions separated by the distance Δ.. If, after the reconstruction of the two images, we place a lens in front of the reconstructed two images, in the focal plane of the lens we will have the Fourier transforms of the two images plus additional square phase factors, namely

$$\begin{aligned}&E(x,y)=\exp\left[\frac{ik}{2f}\left(1-\frac{d}{f}\right)\left(x^2+y^2\right)\right]\times\\ &\mathcal{F}\{U(\xi,\eta)\}(x,y)+\\ &\exp\left[\frac{ik}{2f}\left(1-\frac{d-\Delta}{f}\right)\left(x^2+y^2\right)\right]\times\\ &\mathcal{F}\{U(\xi,\eta)\exp(ik\Delta)\}(x,y)\end{aligned}\quad, \tag{A1}$$

where d is the distance from the first image to the lens f is the focal length of the lens and V is the Fourier transform of U. The phase factor $\exp(ik\Delta)$ is obviously due to the fact that the second image is displaced with Δ with respect to the first image closer to the lens. The power distribution in the focal plane is then

$$\begin{aligned}&I(x,y)=\frac{1}{2}\left|E(x,y)\right|^2=\frac{1}{2}\left|V(x,y)\right|^2\times\\ &\left|\begin{aligned}&\exp\left[\frac{ik}{2f}\left(1-\frac{d}{f}\right)\left(x^2+y^2\right)\right]+\\ &\exp\left[\frac{ik}{2f}\left(1-\frac{d-\Delta}{f}\right)\left(x^2+y^2\right)+ik\Delta\right]\end{aligned}\right|^2=\\ &=\frac{1}{2}\left|V(x,y)\right|^2\left|1+\exp\left[\frac{i\pi\Delta}{\lambda}\left(\frac{r^2}{f^2}+2\right)\right]\right|^2=\\ &\left|V(x,y)\right|^2\left(1+\cos\left[\frac{\pi\Delta}{\lambda}\left(\frac{r^2}{f^2}+2\right)\right]\right)\end{aligned}\quad, \tag{A2}$$

where $V(x,y)$ is the Fourier transform of $U(\xi,\upsilon)$, $r=(x^2+y^2)^{1/2}$ is the radius of the interference rings in the focal plane and λ is the laser wavelength. Since U is a diffusing object, therefore a random distribution of amplitude and phase, so is V. One may notice that we have circles of maximum respectively minimum intensity for

$$\frac{\pi\Delta}{\lambda}\left(\frac{r_m^{\max 2}}{f^2}+2\right)=2m\pi\ , \qquad \text{(A3.a)}$$

$$\frac{\pi\Delta}{\lambda}\left(\frac{r_m^{\min 2}}{f^2}+2\right)=(2m+1)\pi\ , \qquad \text{(A3.b)}$$

where m is a natural number. After some processing the above relation becomes

$$r_m^{\max 2}=2f^2\left(\frac{m\lambda}{\Delta}-1\right),\qquad m\geq\frac{\Delta}{\lambda}, \qquad \text{(A4.a)}$$

$$r_m^{\min 2}=2f^2\left(\frac{(m+1/2)\lambda}{\Delta}-1\right),\qquad m\geq\frac{\Delta}{\lambda}-\frac{1}{2}, \qquad \text{(A4.b)}$$

The relation above may be rewritten in terms on angles, by noting that $\theta\approx r/f$ is the original inclination, before the lens, of the rays that formed the circular fringe of radius r. The difference between the squares of the radii and the inclination of consecutive orders of fringes is a constant

$$\theta_{m+1}^2-\theta_m^2=\frac{r_{m+1}^2-r_m^2}{f^2}=\frac{2\lambda}{\Delta}\ . \qquad \text{(A5)}$$

Similarly, when instead of displacing the object we place a slab of thickness e and refractive index n between the object and the recording medium for the second recording, we have exactly the same results by replacing Δ with $e(n-1)$.

It should be mentioned that scaling considerations like those made in subsection 3.4 apply here as well and they should be used in order to obtain correct values for the radii and the angles.

References

[1] A. W. Lohmann, D. P. Paris, Appl. Opt. **6**, 1739 (1967).

[2] M. Skeren, I. Richter, P. Fiala, Journal of Modern Optics **49**, 1851 (2002)

[3] P. C. Logofatu, D. Apostol, J. Optoelectron. Adv. Mater. **9,** 2838 (2007)

[4] P. C. Logofatu, A. Sima, D. Apostol, Proc SPIE **7297**-04 (2009)

[5] S. Nicolau, D. Apostol, V. Vasiliu, Studii si Cercetari de Fizica **25**, 855 (1973) (in Romanian)

[6] F. Scudieri, M. Bertolotti, A. Ferrari, D. Apostol, Optics Communications **15**, 54 (1975)

[7] D. Apostol, Studii si Cercetari De Fizica, **30**, 779 (1978) (in Romanian)

[8] D. Apostol, Revue Roumaine de Physique **24**, 679 (1979) (in French)

[9] D. Apostol, D. Barbulesku, I. I. Komissarova, G. V. Ostrovskaya, Y. I. Ostrovskii, V. N. Filippov, E. N. Shedova, Zhurnal Tekhnicheskoi Fiziki **58**, 2156 (1988) (in Russian)

[10] D. Apostol, A. Sima, P. C. Logofatu, F. Garoi, V. Nascov, V. Damian, I. Iordache, Proc SPIE **6785**-22 (2007)

[11] C. Wagner, S. Seebacher, W. Osten, W. Jüptner., Appl. Opt. **38**, 4812 (1999)

[12] J. W. Goodman, Introduction to Fourier Optics, McGraw-Hill, New York (1996)

* Corresponding author: petre.logofatu@inflpr.ro